

# Computational analysis of non-coding RNAs in Alzheimer's disease

Ghulam Md Ashraf<sup>1,\*</sup>, Magdah Ganash<sup>2</sup>, Alexiou Athanasios<sup>3,4,\*</sup>

<sup>1</sup>King Fahd Medical Research Center, King Abdulaziz University, P.O. Box 80216, Jeddah 21589, Saudi Arabia; <sup>2</sup>Department of Biology, Faculty of Science, King Abdulaziz University, Jeddah, Saudi Arabia; <sup>3</sup>Novel Global Community Educational Foundation, 7 Peterlee Place, Hebersham, NSW 2770, Australia; <sup>4</sup>AFNP Med, Austria; Ghulam Md Ashraf - E-mail: ashraf.gm@gmail.com; gashraf@kau.edu.sa; \*Corresponding authors

Received March 27, 2019; Accepted April 1, 2019; Published May 15, 2019

DOI: 10.6026/97320630015351

**Abstract:**

Latest studies have shown that Long Noncoding RNAs corresponds to a crucial factor in neurodegenerative diseases and next-generation therapeutic targets. A wide range of advanced computational methods for the analysis of Noncoding RNAs mainly includes the prediction of RNA and miRNA structures. The problems that concern representations of specific biological structures such as secondary structures are either characterized as NP-complete or with high complexity. Numerous algorithms and techniques related to the enumeration of sequential terms of biological structures and mainly with exponential complexity have been constructed until now. While *BACE1-AS*, *NAT-Rad18*, *17A*, and *hnRNP Q* lncRNAs have been found to be associated with Alzheimer's disease, in this research study the significance of the most known  $\beta$ -turn-forming residues between these proteins is computationally identified and discussed, as a potentially crucial factor on the regulation of folding, aggregation and other intermolecular interactions.

**Keywords:** Alzheimer's disease, *BACE1-AS*, *NAT-Rad18*, *17A*, and *hnRNP Q*, long noncoding RNAs, *RAD18*, secondary structure prediction, strict  $\beta$ -turns, structural alignment

**Background:**

Noncoding RNAs (ncRNAs) play important roles in many biological mechanisms offering to the researcher's opportunities for efficient biomarkers' detection and disease diagnosis, treatment, prognosis and prevention [1-3]. While only 1.5% of the whole genome is corresponding to protein-coding genes [1], various Long Noncoding RNAs (lncRNAs) such as *BACE1-AS* are closely related to the Alzheimer's disease (AD) [4-6], modulating  $A\beta$  formation or impacting apoptosis [7-9]. Beta-site Amyloid Precursor Protein Cleaving Enzyme 1 - Antisense Transcript (*BACE1-AS*) enhances *BACE1* mRNA stability by protecting it from degradation [9], concluding to a highly correlation with AD development or progression [5,10-12] as well as *lncRNA-17A* which play a significant role in Gamma-Aminobutyric Acid Type B Receptor Subunit 2 (*GABABR2*) signaling and  $A\beta$  production [7,9].

Additionally, heterogeneous nuclear Ribonucleoprotein Q (*hnRNPs*) family assist in controlling the maturation of newly formed heterogeneous nuclear RNAs (*hnRNAs/pre-mRNAs*) into messenger RNAs (*mRNAs*), stabilize mRNA during their cellular transport and control their translation [13], affecting the dendritic development [14-19]. Latest studies also reveal the role of Postreplication repair protein *RAD18* (*NAT-Rad18*) in AD by affecting the DNA repair system, leading to apoptosis and neurodegeneration [7]. In contrast to protein folding programs, where the tertiary structure is predicted, the majority of the currently available RNA M-folding algorithms concentrate on the secondary structure of the RNA structure. Current RNA prediction algorithms have a polynomial runtime of  $O(n^3)$  where  $n$  is the sequence length. Still, the mere knowledge of the secondary

structure can be misleading, as two similar tertiary structures can have different secondary structures [20]. The problems that concern representations of certain biological structures such as secondary structures are either characterized as NP-complete or with high complexity. The incompleteness of the corresponding theories contributes to a kind of hybrid problem, where data mining, statistical analysis, biological interpretation, and computational techniques must interact in different phases, in order to produce a solution. Numerous algorithms and techniques related to the enumeration of sequential terms of biological structures and mainly with exponential complexity have been constructed through their bijection with alternative representations such as energy models, plane trees and Motzkin numbers, non-crossing set partitions, Motzkin paths and Dyck paths [21]. In contrast to protein folding programs, where the tertiary structure is predicted, the majority of the currently available RNA M-folding algorithms concentrate on the secondary structure of the RNA structure. The first reason for this difference is a pragmatic one. Current RNA prediction algorithms have a polynomial runtime of  $O(n^3)$  where  $n$  is the sequence length. This is fast enough to allow genome-wide analysis on current off-the-shelf computers. The consideration of the tertiary structure, however, leads to a super polynomial-runtime impeding any large-scale application [22]. The second reason is related to the kinetic of RNA folding. Secondary structures form first, leading to a set of loops and helices, which once formed, interact to yield the tertiary structure. As a consequence, the determination of the tertiary structure depends strongly on the secondary structure [23]. Still, the mere knowledge of the secondary structure can be misleading, as two similar tertiary structures can have different secondary structures [20].

## Materials and Methods:

Latest studies have already revealed the correlation between specific lncRNAs to AD pathologies and lesions in brain regions like the middle temporal gyrus, the prefrontal cortex, the striatum the cerebellum and the hippocampus and other CNS related disorders [8, 24-27]. The secondary structures of four proteins related to AD have been examined in this study BACE1, Rad18, GABABR2 and hnRNPQ targeted from the corresponding lncRNAs BACE1-AS, NAT-Rad18, 17A and hnRNP Q [28]. A protein statistics-analysis was initially executed with the QIAGEN CLC Main Workbench (**supplementary material available with authors**). For the computational analysis the sequences 6EJ3(BACE1\_HUMAN), 4F12(GABABR2\_HUMAN), 4UX8 (hnRNPQ\_HUMAN), 2Y43 (RAD18\_HUMAN) were imported from the Protein Databank, avoiding the use of prediction methods for the identification of secondary elements in order to reduce additional errors.

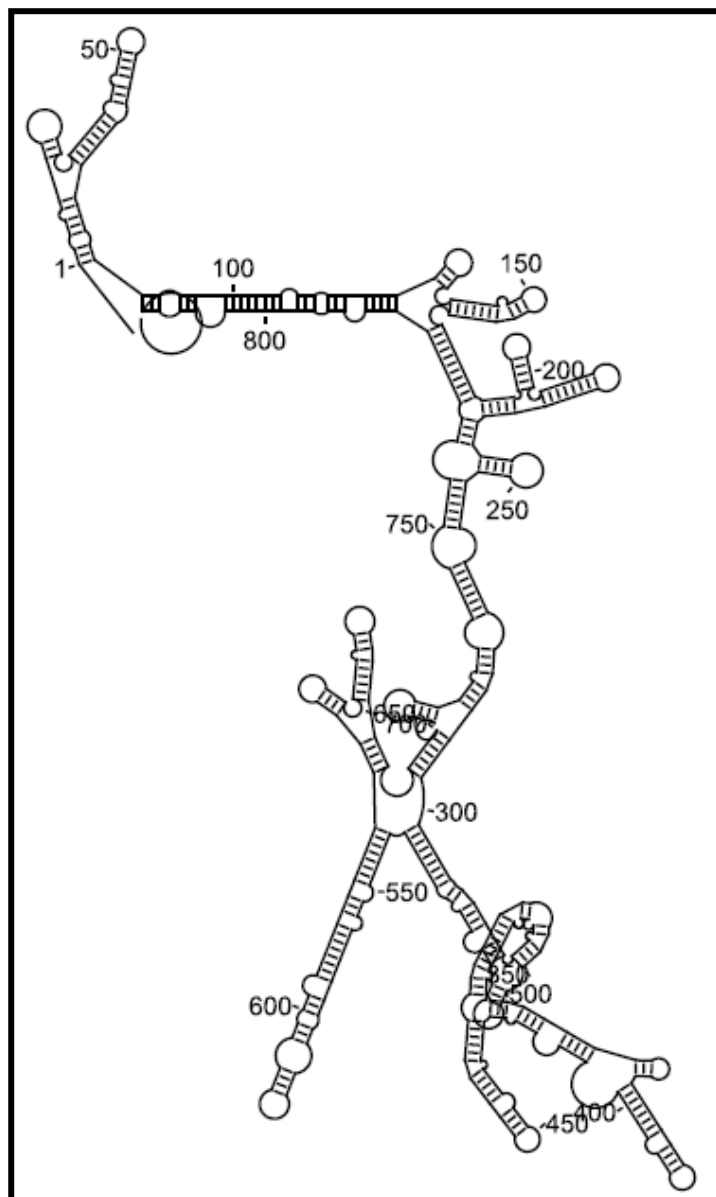


Figure 1: BACE1-AS secondary structure

## Results:

Initially, multiple alignment files have been created using the ClustalOmega software, which has been imported in the ESPrnt 3.0 software for further displaying an analysis of the corresponding secondary structures (Figure 1) [29]. In the ESPrnt output, both the secondary and primary structures are displayed in separate rows, where dots represent gaps,  $\alpha$  stands for alpha helix,  $\beta$  for beta strand, TT for strict  $\beta$ -turns, TTT for strict  $\alpha$ -turns, alpha helices are shown as squiggles and  $\beta$ -strands as arrows in the multiple alignment representation (Figure 2 in supplementary material available with authors), in order to identify similarities and patterns between the proteins.

**Table 1:** Positions of interest with similar properties between BACE1 and GABABR2

Positions	61	62	63	64	65	66
BACE1_HUMAN	V	E	M	V	D	N
Positions	65	66	67	68		
GABR2_HUMAN	T	K	E	V		

Few interesting properties are identified in certain positions of BACE1 and GABABR2 (Table 1). In position (65) there is a decrease in hydrophobicity and a simultaneous increase in the antigenicity of BACE1 (Figure 3). In the corresponding aligned positions of (66,67), there is a decrease in hydrophobicity and antigenicity. Furthermore, in positions (64, 65)  $\beta$ -strict turns to occur in both proteins, while the positions (61-64) of BACE1 have the same levels of hydrophobicity and antigenicity. It is noticed from the computational analysis that  $\beta$ -turns are appeared to be part of the spheroproteins surface and their residues are hydrophilic [30]. Therefore, it seems that in regions with  $\beta$ -turns hydrophobicity is reduced, affecting the folding of each protein and changing the direction of polypeptide's chain (Table 2). In this study, the regions with this interesting property can be found on the common BACE1 and GABABR2  $\beta$ -turns. In positions (64,65) of BACE1 and the corresponding GABABR2 aligned positions, there are identically aligned secondary structures of  $\beta$ -turns. In both turns, hydrophobicity shown to be reduced from a stable state, which confirms the statements concerning the hydrophobicity. In the same region BACE1 and GABABR2 switch from positive to negative hydrophobicity (0.06 to -0.22) and (0.14 to -0.28) respectively. Furthermore, in certain  $\beta$ -turns BACE1 consists of aspartic acid and GABABR2 consists of lysine and glutamic acid which are hydrophilic residues. Although, the  $\beta$ -turns consist of different

residues in general, they still affect the protein folding precisely in the same way. Several research studies since the 70s, underlie the exceptional role of  $\beta$ -turns while they correspond approximately to the 30% of all the protein residues [31-33]. These type of secondary structures are strongly related to protein folding mechanisms depending mainly on their topology, functionality, and stability. According to their classification,  $\beta$ -turns can establish the initiation of folding and in some cases, the substantial destabilization of locally encoded protein features can lead to misfolding [30].

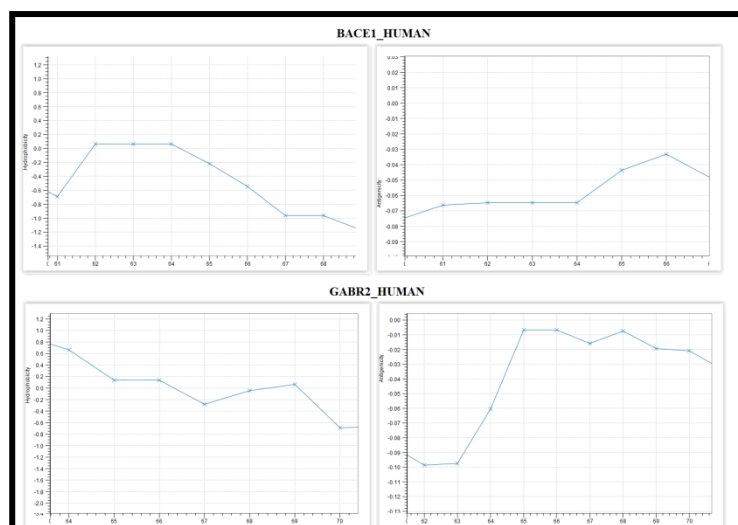


**Figure 3:** Hydrophobicity and antigenicity plots of BACE1 and GABABR2

## Discussion:

A secondary structure  $S$  on a sequence  $s$  is a set of ordered base pairs  $(S_i, S_j)$ , where  $i < j$  and  $s_i$  and  $s_j$  represent respectively the nucleotides at positions  $i$  and  $j$ , on sequence  $s$ , that have the following properties:

- i) If  $(s_i, s_j) \in S$  then  $\{s_i, s_j\} \in \{\{U,A\}, \{G,C\}, \{G,U\}\}$ , where  $\{U,A\}$  and  $\{G,C\}$  are called Watson-Crick pairs and  $\{G,U\}$  is called wobble pair
- ii) If  $(s_i, s_j) \in S$  and  $(s_i, s_l) \in S$  then  $j = l$
- iii) If  $((s_i, s_j) \in S$  and  $(s_k, s_l) \in S$  and  $i < k$  then  $l < j$  or  $j < k$

**Table 2:** The numbers correspond to BACE1. In the case of a gap in BACE1, the number corresponds to GABABR2 with an additional (\*). If there is a gap in both BACE1 and GABABR2, the number corresponds to hnRNPQ with an additional identifier (\*\*)

Regions of interest	Proteins	Structure	High similarity
64-65	BACE1_HUMAN GABR2_HUMAN	Strict $\beta$ -turn Strict $\beta$ -turn	65
67	BACE1_HUMAN HNRPQ_HUMAN	Start of $\beta 1$ Start of $\alpha 1$	67
77-81	HNRPQ_HUMAN RAD18_HUMAN	$\alpha 2$ $\eta 1$ , the start of $\alpha 1$ (81)	79
99	BACE1_HUMAN HNRPQ_HUMAN RAD18_HUMAN	Start of $\beta 4$ Start of $\alpha 3$ End of $\alpha 1$	
106-109	BACE1_HUMAN HNRPQ_HUMAN RAD18_HUMAN	$\beta$ -turn (107-108) end of $\alpha 3$ (106) strict $\alpha$ (107-109)	107 109
118-120	BACE1_HUMAN GABR2_HUMAN RAD18_HUMAN	$\beta$ -turn (119-120) end of $\beta 2$ (119) end of $\beta 1$ (118)	
136*	GABR2_HUMAN RAD18_HUMAN	start of $\alpha 3$ start of strict $\alpha$ -turn	
144*	GABR2_HUMAN RAD18_HUMAN	end of $\alpha 3$ start of $\eta 2$	
149	BACE1_HUMAN GABR2_HUMAN BACE1_HUMAN GABR2_HUMAN	start of strict $\alpha$ -turn end of $\beta 4$ start of $\beta 7$ end of $\eta 2$ (55)	
155-156	HNRPQ_HUMAN RAD18_HUMAN	start of $\alpha 5$ (56) start of $\alpha 4$ $\beta 3$	
173	BACE1_HUMAN GABR2_HUMAN	end of $\beta$ -turn end of $\alpha 5$	
178	BACE1_HUMAN GABR2_HUMAN HNRPQ_HUMAN	start of $\beta 8$ start of $\beta 6$ start of $\alpha 6$	
211	BACE1_HUMAN GABR2_HUMAN	start of $\beta 9$ end of $\beta 7$	
216	BACE1_HUMAN GABR2_HUMAN	end of $\beta 9$ start of $\alpha 7$	
237-240	BACE1_HUMAN GABR2_HUMAN HNRPQ_HUMAN RAD18_HUMAN	end of $\beta 10$ (237) end of $\beta 8$ (239) end of $\alpha 6$ (240) $\beta$ -turn (238-239)	237 239 240
242	BACE1_HUMAN GABR2_HUMAN	start of $\eta 3$ start of $\alpha 8$	
269	BACE1_HUMAN GABR2_HUMAN	end of $\beta 12$ start of $\beta$ -turn	
270	BACE1_HUMAN GABR2_HUMAN	start of $\beta$ -turn end of $\beta$ -turn	
273-274	BACE1_HUMAN GABR2_HUMAN	end of $\beta 13$ (273) start of $\alpha 10$ (274)	
285-286	BACE1_HUMAN GABR2_HUMAN	start of $\beta 14$ (286) end of $\alpha 10$ (285)	
311-312	BACE1_HUMAN GABR2_HUMAN HNRPQ_HUMAN	end of $\alpha 2$ (312) end of $\alpha 11$ (311) start of $\beta$ -turn (312)	312
326-327	GABR2_HUMAN HNRPQ_HUMAN	end of $\beta 11$ (326) start of $\beta$ -turn (327) end of $\alpha 7$ (327)	326 327
330-331	BACE1_HUMAN HNRPQ_HUMAN	end of $\beta 16$ (330) start of $\eta 1$ (331)	331
420*-421*	GABR2_HUMAN	end of $\beta$ -turn (420*)	



	HNRPQ_HUMAN	end of $\eta 1$ (420*) start of $\beta 13$ (421*)	
422*-423*	BACE1_HUMAN GABR2_HUMAN	start of $\beta$ -turn (423*) end of $\beta 13$ (422*)	422
334-335	BACE1_HUMAN GABR2_HUMAN	end of $\beta$ -turn (334) start of $\beta 14$ (335)	334 335
353	BACE1_HUMAN GABR2_HUMAN	start of $\beta$ -turn end of $\beta 15$	
360-361	ACE1_HUMAN GABR2_HUMAN HNRPQ_HUMAN	end of $\beta 18$ (361) end of $\beta 16$ (361) end of $\beta$ -turn (360)	360 361

In other words, constraint i) means that only Watson-Crick and wobble ordered base pairs may form. Constraint ii) states that a nucleotide may be involved in at most one ordered base pair. Constraint iii) implies that all ordered base pairs are nested, i.e. that no pseudoknots are allowed in the secondary structure. While these constraints greatly simplify the folding algorithms, none of the above constraints is biologically relevant. Further pseudoknots appear in many important RNAs structures, albeit at a low frequency. For example, in the small ribosomal unit in E.coli from the 447 reported Watson-Crick and wobble ordered base pairs only 8 are pseudoknots [34]. Any secondary structure generated under these rules can be decomposed into a unique set of a loop [35]. A loop is a substructure which consists of a closing ordered base pair  $(S_i, S_j)$  and all nucleotides that are accessible from this ordered base pair. A nucleotide  $s_p$  is accessible from  $(S_i, S_j)$  if  $i < p < j$  and there exists no other ordered base pair  $(S_k, S_l)$  in S such that  $i < k < p < l < j$ . Loops can be assigned a degree, i.e., the number of ordered base pairs in the loop and size which corresponds to the number of an unpaired nucleotide in the loop. There exist different kinds of loop depending on the amount and arrangement of their interior ordered base pairs [21]. Hairpin loops have a degree of 1. Loops of degree 2 are called interior loops. Interior loops of size zero are called stacked pairs. An uninterrupted sequence of stacked pairs represents a stem. Interior loops of a size larger than 0, with adjacent interior and exterior, ordered base pairs, are called bulge loops. Multiloops are loops of degree greater than 2. Finally, exterior loops are the set of nucleotides which are inaccessible by any ordered base pair. In the literature [36] except for hairpin and interior loops, definitions for bans, multiloops, external loops, pseudoknot loops, interior pseudoknotted loops, and multi-pseudo knotted loops, can also be found. RNA secondary structures can be displayed in different kinds of representations. Depending on the use of the RNA molecules, specific representations are more or less useful. The bracket notation is a text-based representation; the structure is reflected in a string of dots and brackets. Dots denote non-bonding bases and a pair of brackets indicates a base-pair. A more convenient representation, which expands in all directions in

a plane and thus is closer to spatial representation, is the squiggle plot. It is the most prominent plot to easily describe the approximate spatial structure of RNA. Ordered base pairs are given as two bases connected through either a straight line or a circle indicating the so-called wobbling base-pair G-U. Considering RNA secondary structure in a more theoretical way, the representations as trees or as arc-annotated sequences are well-accepted. Schmitt et al computed the total number of RNA secondary structures of a given length with a fixed number of ordered base pairs, under the assumption that all ordered base pairs can occur, by establishing a one-to-one correspondence between secondary structures and trees [37]. In recent years, tree representations of RNA secondary structures occurred in the literature, and algorithmic applications on trees are performed successfully. For example, the full tree representation [38] associates ordered base pairs to internal nodes and unpaired bases to leaf. In a more detailed representation, each interior node is surrounded by right-most and left-most children which correspond to the 5' and 3' nucleotides of the ordered base pair, respectively. In a Shapiro-Zhang tree, the different loops and stacked regions are represented explicitly with special labels [39]. Arc annotated sequences focus on representing sequences as straight lines. Arcs indicate base pairings. A similar representation to the arc-annotated sequence is the drawing of this sequence on a circle. Arcs are plotted as curved lines inside this circle. The mountain plot is useful for large RNAs. Plateaus represent unpaired regions; the heights of these mountains are determined by the number of ordered base pairs in which the partial sequences are embedded. Specifically, the mountain plot representation maps the secondary structure into a 2-dimensional graph where the x-axis represents the position along the RNA sequence and the y-axis corresponds to the number of ordered base pairs that enclose nucleotide k. The dot plot representation maps the structure to a matrix where a dot at position (i, j) represents the ordered base pair  $(S_i, S_j)$ . The secondary structure of an RNA molecule is the collection of ordered base pairs that occur in its 3D structure. When the 5'- end of one nucleotide fits the 3'-end of another, a p-bond is formed, while the sequence of p-bonds defines the backbone of the molecules. On the other hand certain ordered base pairs like {C, G}, {A, U}, and {G, U} form h-bonds, which cause folding of the

molecular backbone into a configuration of minimal energy [40]. In some cases unusual non-canonical ordered base pairs, like {G, U}, {G, A} and {C, A} replace the canonical Watson-Crick ordered base pairs, which maintained a stable helical structure. While these non-canonical pairings allow possible hydrogen-bonding interactions and can be treated as neutral evidence for a helical structure, there seems to be evidence against pairing [41]. A secondary structure of size  $n$  is closed [40] if there is an h-bond connecting base 1 and  $n$  and for known integers  $n \geq 2$ ,  $l \geq 0$ , there are  $S^{(l)}(n-2)$  secondary structures of size  $n$  and rank  $l$ , establishing also a bijection between the set of all closed secondary structures  $Z^{(l)}(n)$  and the set of all plane trees with exactly  $n$  leaves  $T^{(l)}(n)$ .

A constraint satisfaction formulation was also used for RNA prediction problem including genetic mapping [42], physical mapping [43] and structure prediction [44]. The ultimate goal of structure prediction is to obtain the three-dimensional structure of biomolecules through computation. The key concept for solving the above-mentioned problem is the appropriate representation of the biological structures. Nowadays, an increasing number of researchers have released novel RNA structure analysis and prediction algorithms for comparative approaches to structure prediction, based on the fact that closed RNA structures can be viewed as mathematical objects obtained by abstracting topologically non-relevant properties of planar folding of single-stranded nucleic acids. There are a lot of approaches on this topic, such as dynamic programming algorithms [45], stochastic algorithms such as Bioambiens calculus [46], comparative methods [47], simulated annealing [48], artificial neural net algorithms and most recently evolutionary algorithms which attempt to mimic the natural folding pathway by using populations based approach [49].

#### Conclusion:

While specific lncRNAs have been already correlated to certain AD lesions, a new computational analysis of the proteins BACE1, Rad18, GABABR2 and hnRNPQ have been presented in this study. Using the QIAGEN CLC Main Workbench, the ClustalOmega software and the ESPript 3.0 software, a detailed analysis of the corresponding secondary structures for the sequences 6EJ3, 4F12, 4UX8, 2Y43 has been executed. The results of our computational analysis identified common properties in aligned positions with high similarity score, identical secondary structure match, increased hydrophilicity, and negative antigenicity, revealing simultaneously strong evidence that the proteins under consideration, may have common functionality in those regions that regulate folding and aggregation and prevent binding of immune factors. These conclusions reveal the significance of the most known  $\beta$ -turn-forming residues, which participate in ligand

binding, molecular recognition, protein-protein or protein-nucleic acid interactions and modulation of protein functions and intermolecular interactions, in proteins commonly linked to AD development or progression.

#### Acknowledgment:

This project was funded by the Deanship of Scientific Research (DSR) at King Abdulaziz University, Jeddah, under the grant No. (G-670-141-39). The authors, therefore, acknowledge with thanks DSR for technical and financial support.

**Conflict of interest:** There is no conflict of interest.

#### References:

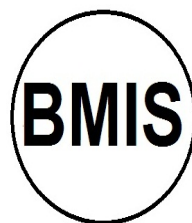
- [1] Chen X *et al.* *Briefings in Bioinformatics* 2017 **18**:558 [PMID: 27345524]
- [2] Zhang Y *et al.* *BioMed Research International* 2017 **2017**:1 [PMID: 9139504]
- [3] Backofen R *et al.* *Methods in Molecular Biology* 2018 **1704**:363 [PMID:29277874]
- [4] Mus E *et al.* *Proc Natl Acad Sci USA* 2007 **104**: 10679 [PMID: 17553964]
- [5] Faghihi M *et al.* *Nat. Med.* 2008 **14**:723 [PMID:18587408]
- [6] Ng SY *et al.* *Trends Genet* 2013 **29**:461 [PMID: 23562612]
- [7] Parenti R *et al.* *Eur J Neurosci.* 2007 **26**:2444 [PMID:17970741]
- [8] Luo Q *et al.* *Clinical Interventions in Aging* 2016 **11**:867 [PMID:27418812]
- [9] Kim J *et al.* *Biochimica et Biophysica Acta* 2016 **1859**:209 [PMID:26141605]
- [10] Fukumoto H *et al.* *Arch. Neurol.* 2002 **59**:1381 [PMID:12223024]
- [11] Faghihi M *et al.* *Genome Biol.* 2010 **11**:1 [PMID:20507594]
- [12] Modarresi F *et al.* *Int. J. Alzheimers Dis.* 2011 **2011**: 1 [PMID:21785702]
- [13] Dreyfuss G *et al.* *Cell.* 1996 **85**:963 [PMID: 8674124]
- [14] Mourelatos Z *et al.* *EMBO J.* 2001 **20**:5443 [PMID:11574476]
- [15] Chen HH *et al.* *Mol Cell Biol.* 2008 **28**:6929 [PMID: 18794368]
- [16] Xing L *et al.* *Mol Biol Cell.* 2012 **23**:6929 [PMID: 22357624]
- [17] Svitkin YV *et al.* *PLoS Biol.* 2013 **11**:1 [PMID: 23700384]
- [18] Williams KR *et al.* *Mol Biol Cell* 2016 **27**:518 [PMID: 26658614]
- [19] Geuens T *et al.* *Human Genetics* 2016 **135**:851 [PMID:27215579]
- [20] Krasilnikov AS *et al.* *Science* 2004 **306**:104 [PMID: 15459389]
- [21] Hofacker I *et al.* *Discrete Applied Mathematics* 1998 **88**:207
- [22] Akutsu T *Discrete Applied Mathematics* 2000 **104**:45
- [23] Brion P *et al.* *Annual Review of Biophysics and Biomolecular Structure* 1977 **26**:113 [PMID: 9241415]
- [24] Idda M *et al.* *Wiley Interdisciplinary Reviews RNA* 2018 **9**:1 [PMID:29327503]

- [25] Kim Y *et al.* *Journal of Clinical Medicine* 2018 **7**:1 [PMID:30469430]
- [26] Zhou M *et al.* *Briefings in Bioinformatics* 2018 [PMID: 29672663]
- [27] Wei CW *et al.* *Front. Behav. Neurosci.* 2018 **12**:1 [PMID: 30323747]
- [28] Quan Z *et al.* *Frontiers in Cellular Neuroscience* 2017 **11**:1 [PMID: 28713244]
- [29] Robert X *et al.* *Nucleic Acids Res.* 2014 **42**: 320 [PMID: 24753421]
- [30] Marcelino AM *et al.* *Biopolymers* 2008 **89**: 380 [PMID: 18275088]
- [31] Sammon J *IEEE Transactions on Computers* 1969 **18**: 401
- [32] Chou PY *et al.* *Journal of Molecular Biology* 1977 **115**: 135 [PMID: 592361]
- [33] de Brevern A *Sci. Rep.* 2016 **6**:1 [PMID:27627963]
- [34] Gutell R *et al.* *Proceedings of the National Academy of Sciences* 1990 **87**: 663 [PMID:2300554]
- [35] Matthews RT *et al.* *Neuroscience* 1991 **42**: 451 [PMID: 1680227]
- [36] Rastegari B *et al.* *Algorithms in Bioinformatics.* WABI 2005. LNCS Springer **3692**: 341
- [37] Schmitt WR *et al.* *Discrete Applied Mathematics* 1994 **51**: 317
- [38] Fontana W *et al.* *Biopolymers* 1993 **33**: 1389 [PMID: 7691201]
- [39] Shapiro B, *Comput Appl Biosci.* 1988 **4**: 387 [PMID: 2458170]
- [40] Došlić T *et al.* *Discrete Mathematics* 2004 **285**: 67
- [41] Chen J *et al.* *Cell* 2000 **100**: 503 [PMID: 10721988]
- [42] Letovsky S *et al.* *Genomics* 1992 **12** 435 [PMID:1559695]
- [43] Yap IV *et al.* *Genetics* 2003 **165**: 2235 [PMID: 14704199]
- [44] Gaspin C *et al.* *Journal of Molecular Biology* 1995 **254**: 163 [PMID:7490740]
- [45] Zuker M *Science* 1989 **244**: 48 [PMID: 2468181]
- [46] Regev A *et al.* *Theoretical Computer Science* 2004 **325**: 141
- [47] Mathews D *et al.* *Journal of Molecular Biology* 2002 **317**: 191 [PMID:11902836]
- [48] Schmitz M *et al.* *Computer Applications in the Biosciences: CABIOS* 1992 **8**:389
- [49] Wiese K *et al.* *Biosystems* 2003 **72**:29 [PMID: 14642657]

Edited by P Kanguane

Citation: Ashraf *et al.* *Bioinformation* 15(5): 351-357 (2019)

**License statement:** This is an Open Access article which permits unrestricted use, distribution, and reproduction in any medium, provided the original work is properly credited. This is distributed under the terms of the Creative Commons Attribution License



Biomedical Informatics Society

Agro Informatics Society



# Journal